Magnetic properties and spin dynamics in the single-molecule paramagnets Cu_6Fe and Cu_6Co

P. Khuntia,[1,2] M. Mariani,[1,3] M. C. Mozzati,[1] L. Sorace,[4] F. Orsini,[3,5] A. Lascialfari,[1,3,5,*] F. Borsa,[1] C. Maxim,[6] and M. Andruh[6]

[1]*Dipartimento di Fisica "A.Volta" e Unita' CNISM-CNR, Universita' di Pavia, I-27100 Pavia, Italy*

[2]*Department of Physics, Indian Institute of Technology Bombay, Powai, Mumbai 400076, India*

[3]*S3-CNR-INFM, I-41100 Modena, Italy*

[4]*Laboratory for Molecular Magnetism and INSTM Research Unit, University of Florence, I-50019 Sesto Fiorentino, Italy*

[5]*Dipartimento di Scienze Molecolari Applicate ai Biosistemi, DISMAB, Università di Milano, I-20134 Milano, Italy*

[6]*Inorganic Chemistry Laboratory, Faculty of Chemistry, University of Bucharest, Str. Dumbrava Rosie 23, 020464 Bucharest, Romania*

(Received 24 April 2009; published 21 September 2009)

The magnetic properties and the spin dynamics of two molecular magnets have been investigated by magnetization and dc susceptibility measurements, electron paramagnetic resonance and proton nuclear magnetic resonance (NMR) over a wide range of temperatures (1.6–300K) at applied magnetic fields $H=0.5$ and 1.5 T. The two molecular magnets consist of $Cu^{II}(saldmen)(H_2O)\}_6\{Fe^{III}(CN)_6\}](ClO_4)_3\cdot 8H_2O$ in short Cu_6Fe (here H saldmen is the Schiff base resulted by reacting salicylaldehyde with N,N-dimethylethylenediamine) and the analog compound with cobalt, Cu_6Co. It is found that in Cu_6Fe, whose magnetic core is constituted by six Cu^{2+} ions and one Fe^{3+} ion all with $s=1/2$, a weak ferromagnetic interaction between Cu^{2+} moments through the central Fe^{3+} ion with $J=0.14$ K is present, while in Cu_6Co the Co^{3+} ion is diamagnetic and the weak interaction is antiferromagnetic with $J=-1.12$ K. The NMR spectra show the presence of nonequivalent groups of protons with a measurable contact hyperfine interaction consistent with a small admixture of *s* wave function with the *d* function of the magnetic ion. The NMR relaxation results are explained in terms of a single-ion (Cu^{2+}, Fe^{3+}, Co^{3+}) uncorrelated spin dynamics with an almost temperature-independent correlation time due to the weak magnetic exchange interaction. We conclude that the two molecular magnets studied here behave as single-molecule paramagnets with a very weak intramolecular interaction, almost on the order of the dipolar intermolecular interaction. Thus they represent a separate class of molecular magnets which differ from the single-molecule magnets investigated up to now, where the intramolecular interaction is much larger than the intermolecular one.

DOI: 10.1103/PhysRevB.80.094413 PACS number(s): 75.50.Xx, 76.60.−k, 75.50.Ee

I. INTRODUCTION

The development of molecular chemistry in synthesizing transition metal-ion-based molecular clusters whose properties are midway between atoms and bulk systems provides a unique opportunity to the scientific community for the study of nanoscale magnetism.[1] Because of the presence of nonmagnetic organic ligands that prevent magnetic interactions, the intermolecular interactions are weak in comparison to intramolecular superexchange interactions. Hence, the molecules are isolated magnetically from each other and it is of great interest to investigate spin dynamics of these nanomagnets, often called single-molecule magnets (SMM). In the SMM reported up to now, a strong exchange magnetic interaction exists among the magnetic moments within each individual molecule which leads to a low-temperature ground state characterized by either a high total moment *S* or a singlet antiferromagnetic (AFM) state $S=0$ depending on the topology of the magnetic ions and on their mutual magnetic coupling. In the case of high spin ground state and high magnetic anisotropy, quantum tunneling of magnetization and quantum coherence at low temperature have been observed, making these nanomagnets promising candidates for magnetic storage and quantum computing among other applications.[2,3]

In this paper we present the magnetic properties of heptanuclear molecular magnets Cu_6Fe and Cu_6Co with very small intramolecular magnetic coupling. These molecules are thus a prototype of single-molecule paramagnets. As it will be shown by the experimental results, the Cu_6Fe compound consists of six Cu^{2+} magnetic ions with a weak ferromagnetic interaction via the bond to a central Fe^{3+} ion. The isostructural Cu_6Co compound, instead, appears to be formed by six Cu^{2+} magnetic ions and a central diamagnetic Co^{3+} ion with a small antiferromagnetic coupling between Cu^{2+} ions via the bond to the central Co^{3+} ion (Fig. 1).

The paper is organized as follows. In Sec. II we summarize briefly the synthesis of the compounds and their crystal structure. The detailed description of the results of this section will be presented in a separate publication.[4] In Sec. III we present the experimental results and data analysis. The results are presented in separate subsections for the magnetization, the electron paramagnetic resonance (EPR), the static and the dynamic NMR. Section IV contains a comparison between Cu_6Fe and Cu_6Co and a discussion of the results obtained with the different techniques and the relevant conclusions.

II. THE SAMPLES

A. Cu_6Fe

Polycrystalline sample $[\{Cu^{II}(saldmen)(H_2O)\}_6\{Fe^{III}(CN)_6\}](ClO_4)_3\cdot 8H_2O$ (i.e., $C_{72}H_{118}C_{13}Cu_6FeN_{18}O_{32}$)

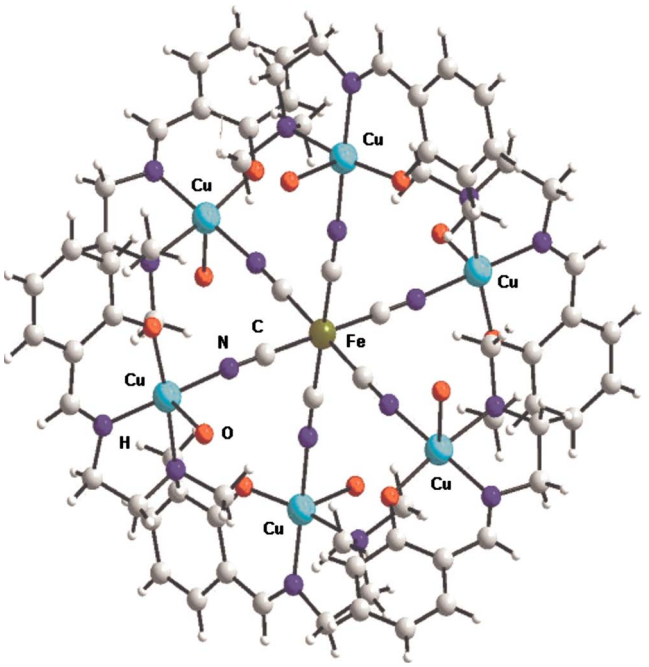

FIG. 1. (Color online) Crystal structure of Cu_6Fe. Cu_6Co is isostructural, with Fe replaced by Co.

was synthesized from the reaction of binuclear copper(II) complex, $[Cu_2(saldmen)_2(\mu\text{-}H_2O)(H_2O)_2](ClO_4)_2\cdot 2H_2O$, with $K_4[Fe(CN)_6]$ (H saldmen is the Schiff base resulted by reacting salicylaldehyde with N,N-dimethylethylenediamine as will be described elsewhere[4]). In this molecule, 16 out of 118 protons belong to 8 crystallization water molecules and the remaining 102 protons arise from the organic ligands and from six water molecules coordinated to six Cu^{2+} ions.

The lattice is of hexagonal symmetry (R-3c) with cell constants $a=27.8777(16)$ Å, $b=27.8777(16)$ Å, $c=21.369(13)$ Å, $\alpha=\beta=90°$, and $\gamma=120°$. The six Cu^{2+} ions are located at the corners of an octahedron and are connected by the cyano groups and one Fe^{3+} at the center of the octahedron. The Cu-Fe-Cu angles are 180° and the Fe-Cu angles across the CN bridges are Cu-N-C=171.76(54)° and Fe-C-N=176.54(57)°.

The nearest neighbor bond distances are Fe-H =4.0482 Å and Cu-H=2.9649 Å.

B. Cu_6Co

The Cu_6Co crystals were obtained by adding an acetonitrile-water (1:1) solution (20 mL) containing 0.3 mmol of $[Cu_2(saldmen)_2(\mu\text{-}H_2O)(H_2O)_2](ClO_4)_2\cdot 2H_2O$, 10 mL acetonitrile-water (1:1) solution containing 0.1 mmol of $K_3[Co(CN)_6]$ under stirring. Green crystals suitable for x-ray diffraction were obtained directly from the reaction mixture, by slow evaporation of the filtrate at room temperature.[4]

The lattice is also of hexagonal symmetry (R-3c) with cell constants $a=27.9545(19)$ Å, $b=27.9545(19)$ Å, $c=21.3938(16)$ Å, $\alpha=\beta=90°$, and $\gamma=120°$. The six Cu^{2+} ions are located at the corners of an octahedron and are connected by the cyano groups and one Co^{3+} at the center of the octahedron. The Cu-Co-Cu angles are 180° and the Co-Cu angles across the CN bridges are Cu-N-C=174.21° and Co-C-N=173.712°.

The nearest-neighbor bond distances are Co-H =3.9836 Å and Cu-H=2.9628 Å.

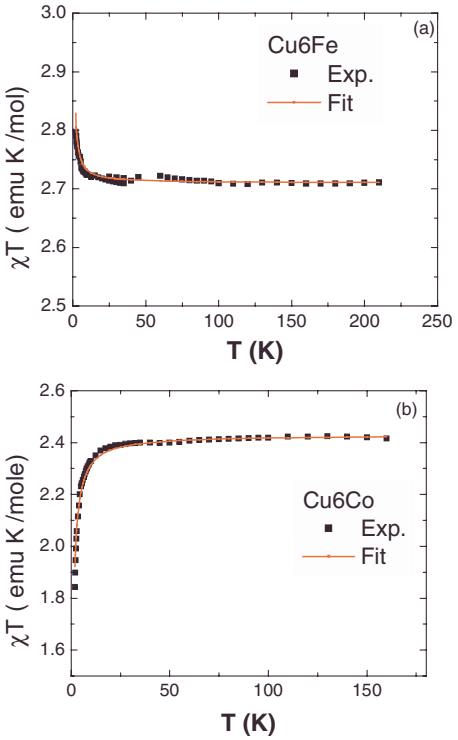

FIG. 2. (Color online) Magnetic susceptibility times the temperature vs temperature for (a) Cu_6Fe and (b) Cu_6Co. The solid lines are theoretical fits in terms of a Curie-Weiss law as discussed in the text.

III. EXPERIMENTAL RESULTS AND ANALYSIS

A. Magnetic susceptibility

The temperature dependence of the magnetic susceptibility ($\chi=M/H$) in the temperature range 2–210 K at two applied magnetic fields, 0.1 and 1 T for Cu_6Fe, and in the temperature range 2–160 K at 1 T for Cu_6Co, was measured with a superconducting quantum interference device (SQUID) magnetometer. The raw data were corrected by the sample holder and the single-ion diamagnetic contributions before analysis.

The results of the susceptibility measurements are shown in Fig. 2 for both Cu_6Fe and Cu_6Co samples. Over most of the temperature range the χT vs T data show a simple paramagnetic behavior. At very low temperature the departure is evident from the simple Curie law due to a small ferromagnetic (FM) coupling for Cu_6Fe and a small AFM coupling for Cu_6Co.

The data for Cu_6Fe can be fitted with a Curie-Weiss law with $C=2.72\pm0.2$ (emu K/mol) and $T_C=+0.07$ K. This corresponds to an average g factor for the seven spins $s=1/2$ per molecule of $g=2.035$. This is surprisingly low, given the supposedly unquenched orbital momentum characterizing the $^2T_{2g}$ state of low spin Fe(III) in octahedral sym-

metry which should lead to a much larger average g value.[5] The same behavior has been recently reported for a linear, cyanide bridged, CuFeCu complex, and attributed to the peculiar geometrical distortion of $Fe(CN)_6$ unit, leading to an almost complete quench of the angular momentum.[6] The obtained value of the Weiss constant correspond, in the framework of simple molecular-field approximation (MFA), $\theta = \frac{2zs(s+1)J_F}{3k_B}$, to a weak ferromagnetic interaction $J_F = 0.14$ K (here z is the number of nearest neighbors).

On the other hand the data for Cu_6Co were fitted with a Curie-Weiss law with $C = 2.44 \pm 0.06$ (emu K/mol) and $T_N = -0.56$ K. This corresponds to six spins $s = 1/2$ with an average g factor $g = 2.075$. Again, by using the MFA expression for the Weiss constant one finds an antiferromagnetic interaction $J_{AF} = -1.12$ K.

As a whole, these results point to the existence of only a very weak exchange coupling interaction between the magnetic centers. This conclusion is reinforced by the isothermal magnetization curves which can be fitted reasonably well in terms of noninteracting paramagnetic ions.[4]

While this is not much surprising for the Cu_6Co derivative, for which the interacting centers are located far apart from each other, and mutually counterbalancing interactions may occur, the situation is more puzzling for the Cu_6Fe derivative. For this system the magnetic orbitals of Cu(II) and those of Fe(III), respectively, e_g and t_{2g} in octahedral symmetry, should be orthogonal, leading to a substantial ferromagnetic interaction. While the observed interaction is indeed of the expected sign, its magnitude is much lower than expected. It is, however, to be noted that a negligibly small value of the exchange coupling of Cu(II) with $Fe(CN)_6^{3-}$ units has been recently reported.[7]

B. EPR spectra

EPR measurements were carried out at 9.45 GHz (X band) at room temperature with a Bruker spectrometer, equipped with a standard microwave cavity. A modulation field of 0.05 mT and a microwave power of about 1.86 mW were used.

The room temperature EPR spectrum of Cu_6Fe and Cu_6Co are shown in Fig. 3. The shape of the signal for both systems is typical of octahedral Cu^{2+} ions with axial distortion environment, leading to a $g_\parallel > g_\perp > 2.00$ pattern. This is in agreement with the findings of crystal-structure solution, which indicated a square pyramidal coordination environment for Cu(II).[8] The experimental spectrum could be satisfactorily simulated (as a powder spectrum resulting from the superposition of spectra of axial sites with angular orientations randomly distributed) by assuming an anisotropic g factor with a Lorentzian line shape. The values obtained from the simulation of the spectrum are $g_\parallel = 2.172$ and $g_\perp = 2.085$. This confirms that the unpaired electron is located, as expected, in a $d_{x^2-y^2}$ orbital, so that the absence (or weakness) of the exchange coupling between Fe(III) and Cu(II) should be regarded as accidental. Finally, we note that the absence of the EPR signal arising from Fe^{3+} ion in the corresponding derivative at room temperature is most likely due to the fast relaxation time of low spin Fe(III) at this temperature, leading to an exceedingly broad line. Further studies at lower temperatures are currently in progress to clarify this issue.

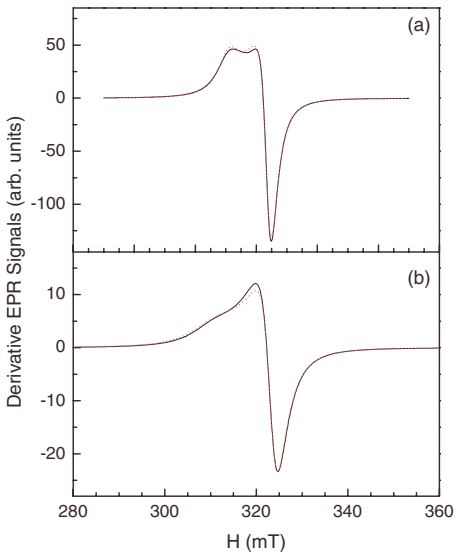

FIG. 3. (Color online) Experimental (black line) and computed from numerical analysis (dotted gray line, red in online version) derivative EPR signals in (a) Cu_6Fe and (b) Cu_6Co.

C. Proton NMR spectra

Nuclear magnetic resonance (NMR) measurements on polycrystalline Cu_6Fe and Cu_6Co samples were performed with a standard TecMag Fourier transform pulse NMR spectrometer using short $\pi/2$-$\pi/2$ radio frequency (rf) pulses (1.9–2.2 μs) in the temperature range 1.6–300 K at two applied magnetic fields, $H = 0.5$ and 1.5 T. We employed a continuous flow cryostat in the temperature range 4.2–300 K and a bath cryostat in the temperature range 1.6–4.2 K. Fourier transform of the half echo spin signal of the NMR spectrum was taken in the case where the whole line could be irradiated with one rf pulse. The low-temperature broad spectra were obtained by the convolution of lines obtained from several Fourier transforms each one collected at different values of the irradiation frequency keeping the external field constant.

Proton NMR spectra for Cu_6Fe and Cu_6Co were collected as a function of frequency at constant applied magnetic field $H = 1.5$ T at different temperatures. The spectra thus obtained are shown in Fig. 4. They are found to broaden progressively with decreasing temperature and to develop a structure due to the presence of a shifted small component. The spectra at low temperatures could be fitted well with two Gaussian functions having different width and shift. In the analysis of the data which follows we use as experimental results for the full width at half maximum (FWHM) and for the paramagnetic shift $K_{ps} = \frac{\Delta\nu}{\nu_L}$ (ν_L is the Larmor frequency) the values used for the fitted Gaussian lines.

The shape and width of the proton NMR spectrum are determined by two main interactions: (i) the nuclear-nuclear dipolar interaction, (ii) the hyperfine interaction of the proton with the neighboring magnetic ions. The first interaction gen-

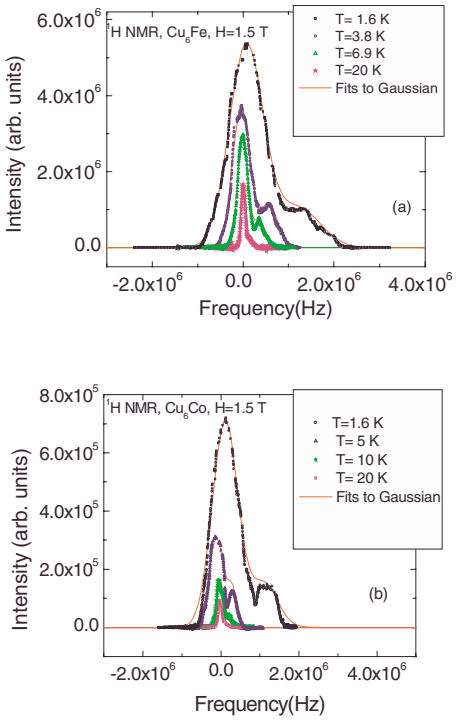

FIG. 4. (Color online) Representative spectra of proton NMR at different temperatures with fitting curves made up of the superposition of two Gaussian lines at different resonance frequency for (a) Cu_6Fe and (b) Cu_6Co.

erates a temperature- and field-independent broadening[9] which depends on the hydrogen distribution in the molecule and is thus similar in all molecular magnets independently of their magnetic properties.[10]

The hyperfine field resulting from the interaction of protons with local magnetic moments of Cu^{2+} may contain contributions from both the classical dipolar interaction and from a direct contact term due to the hybridization of proton *s* wave function with the *d* wave function of magnetic ions. The dipolar contribution has tensorial character and is thus responsible for the inhomogeneous width of the line due to the random distribution of orientations in a powder sample and to the many nonequivalent proton sites. The contact interaction, on the other hand, has scalar form and it can generate a shift of the line for certain groups of equivalent protons in the molecule.[11]

In the usual simple Gaussian approximation for the NMR line shape, the linewidth is proportional to the square root of the second moment, which in turn is given by the sum of the second moments due to the two interactions described above[9]

$$\mathrm{FWHM} \propto \sqrt{\langle \Delta\nu^2 \rangle_d + \langle \Delta\nu^2 \rangle_m}, \tag{1}$$

where $\langle \Delta\nu^2 \rangle_d$ is the intrinsic second moment due to nuclear dipolar interactions, and $\langle \Delta\nu^2 \rangle_\mathrm{m}$ is the second moment of the local frequency-shift distribution (due to nearby electronic moments) at the different proton sites of all molecules. The relation between $\langle \Delta\nu^2 \rangle_m$ and local Cu^{2+} electronic moments for a simple dipolar interaction is given by[9]

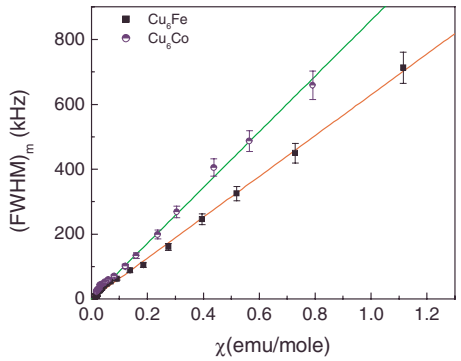

FIG. 5. (Color online) Magnetic inhomogeneous broadening of the proton NMR line plotted vs magnetic susceptibility in Cu_6Co and Cu_6Fe. The straight lines are curve fits according to Eq. (3).

$$\langle \Delta\nu^2 \rangle_m = \frac{1}{N}\sum_R \Big(\sum_{i\in R} \langle \nu_{R,i} - \nu_0 \rangle_{\Delta t}\Big)^2 = \frac{\gamma^2}{N}\sum_R \left[\sum_{i\in R}\sum_{j\in R} \frac{A(\vartheta_{i,j})}{r_{i,j}^3}\langle m_{z,j}\rangle_{\Delta t}\right]^2, \tag{2}$$

where *R* labels different molecules, *i* and *j* span different protons and Cu^{2+} ions within each molecule, and *N* is the total number of probed protons. In Eq. (2), $\nu_{\mathrm{R,i}}$ is the NMR resonance frequency of nucleus *i* and $\nu_L = \gamma H/2\pi$ is the bare Larmor resonance frequency. The difference between the two resonance frequencies represents the shift for nucleus *i* due to the local field generated by the nearby moments *j*. A $(\vartheta_{\mathrm{i,j}})$ is the angular-dependent dipolar coupling constant between nucleus *i* and moment *j* and $r_{\mathrm{i,j}}$ the corresponding distance. $\langle m_{\mathrm{z,j}} \rangle$ is the component of the Cu^{2+} moment *j* in the direction of the applied field, averaged over the NMR data acquisition time scale. In a simple paramagnet one expects $\langle m_{z,j}\rangle = \frac{\chi}{N_A}$, where χ is the SQUID susceptibility in emu/mole and $\mathrm{N_A}$ is Avogadro's number. We can thus write approximately

$$\mathrm{FWHM} = \sqrt{\langle \Delta\nu^2 \rangle_m} = A_z\chi, \tag{3}$$

where A_z is the dipolar coupling constant averaged over all protons and all orientations.

The experimental results for the magnetic contribution to the linewidth are plotted as a function of the magnetic susceptibility in Fig. 5 for both Cu_6Fe and Cu_6Co. The linear relation predicted by Eq. (3) is well verified and the values obtained from the fit for the average dipolar coupling are $A_z = 2.53 \times 10^{22}$ cm^{-3} (for Cu_6Fe) and $A_z = 3.44 \times 10^{22}$ cm^{-3} (for Cu_6Co) which are consistent with the dipolar interaction of protons not directly coupled to the Cu^{2+} magnetic ions at a mean distance of 3 Å from Cu^{2+}.

We turn now to the analysis of the small shifted line observed in the NMR spectra of both Cu_6Fe and Cu_6Co (see Fig. 4). The paramagnetic shift is defined as $K_{ps} = \frac{\nu_R - \nu_L}{\nu_L}$, where ν_R is the resonance frequency and ν_L is the proton Larmor frequency. It can be expressed as[11]

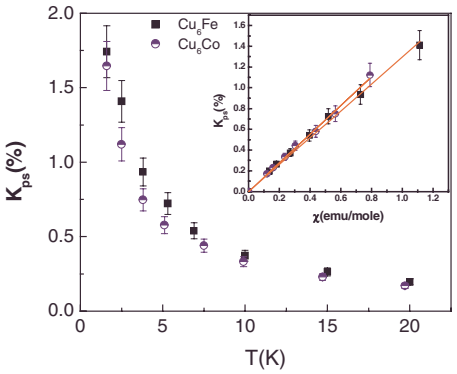

FIG. 6. (Color online) Temperature dependence of paramagnetic shift of the satellite line (see Fig. 4) in Cu_6Fe and Cu_6Co. The inset shows the linear behavior of K_{ps} vs χ with temperature as an implicit parameter.

$$K_{ps} = \frac{H_{\text{eff}}}{N_A \mu_B} \chi(T), \tag{4}$$

where μ_B=Bohr magneton and $\chi(T)$=paramagnetic susceptibility per mole, N_A=Avogadro's number, H_{eff}=local hyperfine field. The hyperfine field, which generates the line shift, is due to a contact scalar interaction arising from the electron density associated with the s part of the wave function at the proton site. Thus H_{eff} can be expressed in terms of the atomic hyperfine coupling constant, $a(s)$, multiplied by a correction factor, ξ, which gives the fraction of s character of the wave function of the magnetic electron at the proton site[11]

$$H_{\text{eff}} = \mu_B \xi a(s). \tag{5}$$

For an atom the hyperfine constant can be expressed as $a(s) = \frac{16\pi}{3} \gamma_n \hbar \mu_B P_A$, with $P_A = |\psi_A(0)|^2$ the electron probability density at the nucleus for the free atom.

The experimental results for the shift of the satellite line in Fig. 4 are shown in Fig. 6 for both Cu_6Fe and Cu_6Co plotted also as a function of the magnetic susceptibility. As seen in the figure the prediction of Eq. (4) is well verified. From the slope of the plot of the shift vs the susceptibility one derives a value of 50.65 mT for the hyperfine magnetic field at the proton site for hydrogen bonded to the Cu^{2+} for Cu_6Fe and a value of 46.24 mT in the case of Cu_6Co.

The theoretical hyperfine constant for H atom is $a(s) = 0.0473$ cm^{-1} (Ref. 11) close to the value reported for the molecular hydrogen ion H_2^+ (Ref. 12) and corresponding to a hyperfine field at the proton site of about 28 T. Thus the contact term for the bridging hydrogen's in Cu_6Fe and Cu_6Co is only about 0.17% of the atomic hyperfine field for $1s$ electron in hydrogen atom consistent with a very small overlap of d and s wave functions of the magnetic ion and the hydrogen, respectively.

D. Proton NMR signal intensity, T_2 and wipeout effects

The normalized signal intensities for protons studied as a function of temperature in Cu_6Fe and Cu_6Co are shown in Fig. 7. The signal intensity was measured by the area under the echoes collected at different delay times, obtained from the usual Hahn-echo sequence.[13] To obtain the normalized signal intensity the $M_{xy}(t)$ vs t curve giving the spin-spin relaxation recovery law was extrapolated at $t=0$ and normalized by multiplying by T to compensate for the Boltzmann factor. At low temperature the spectrum broadens and so it was acquired point by point by sweeping the resonance frequency at fixed magnetic field. As shown in Fig. 7 the decrease of the normalized intensity in the intermediate temperature regime indicates a loss of signal. The loss of signal is a phenomenon, which has been observed in many molecular nanomagnets.[14] The explanation of this "wipeout" effect rests in the very short T_2 attained by the nuclei closer to the magnetic ions. T_2 was measured in our systems from the exponential decay of the echo amplitude as a function of time delay between two rf pulses and the results are shown in Fig. 8. The very short value of T_2 and the broad maximum observed in the T dependence of $1/T_2$ in Fig. 8 are in qualitative agreement with the loss of signal intensity observed in the same temperature range.

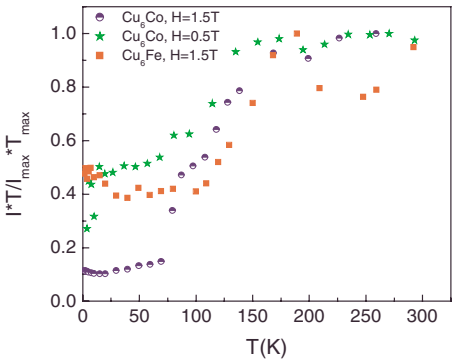

FIG. 7. (Color online) Temperature dependence of normalized NMR signal intensity multiplied by temperature

Thus the results of the temperature and field dependence of the relaxation rate, which will be discussed in the following paragraph, refer only to the average proton relaxation rate of the nuclei which can be detected. Since a large number of nuclei escapes detection (i.e., the above cited wipeout effect) the absolute values of $1/T_1$ are clearly not very significant. However, the relative temperature and field dependence should not be affected by the wipeout effect.

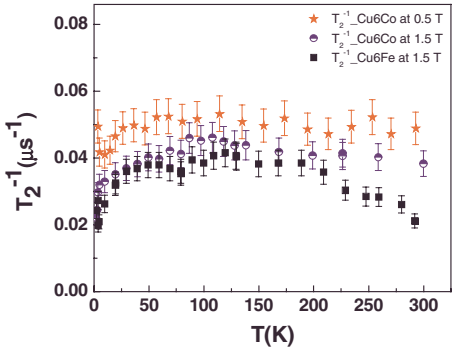

FIG. 8. (Color online) Temperature dependence of spin-spin relaxation rate in Cu_6Fe at $H=1.5$ T and at $H=1.5$ T and at $H=0.5$ T in Cu_6Co.

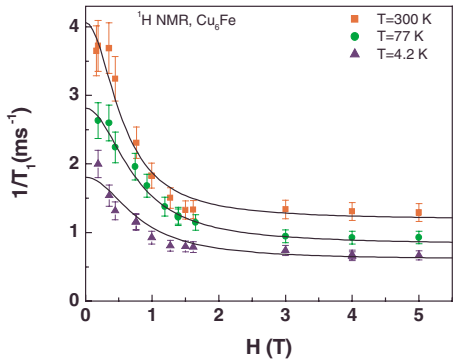

FIG. 9. (Color online) Field dependence of spin-lattice relaxation rate in Cu_6Fe at various temperatures with fit according to Eq. (7) (see text).

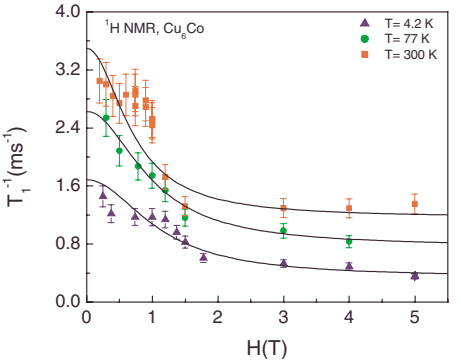

FIG. 10. (Color online) Field dependence of spin-lattice relaxation rate in Cu_6Co at various temperatures with fit according to Eq. (7) (see text).

E. Temperature and field dependence of NSLR

The proton nuclear spin-lattice relaxation rate (NSLR), T_1^{-1}, was obtained by monitoring the recovery of the nuclear magnetization following a long comb of $\pi/2$ rf pulses in order to obtain the best initial saturation conditions. The recovery was found to be strongly nonexponential at all temperatures and magnetic fields. This is a common situation in molecular nanomagnets[10] since the protons are located at different distances and angles from the relaxing magnetic ions. Since the spin diffusion is not sufficiently fast to ensure a common spin temperature during the recovery process, the recovery curve is a superposition of many exponential curves each one representing the relaxation of a given proton. By measuring the initial recovery or tangent at the origin one measures the average relaxation rate, which is dominated by the fast relaxing protons (the nearest to the magnetic ions). The shape of the recovery curve may change as a function of temperature and magnetic field as the result of the spin-diffusion effect.[15] Thus for better consistency we measured the NSLR from the time at which the recovery curve has reduced to $1/e$ of the initial value. The measured parameter is in any case proportional to the average relaxation rate of the protons detected in the NMR signal.[15]

The results for the field dependence of the proton relaxation rate at three different temperatures in both compounds are shown in Figs. 9 and 10. The results for the temperature dependence of proton NSLR at two external magnetic fields, $H=1.5$ and 0.5 T are shown in Fig. 11.

The weak temperature dependence is at variance with the pronounced peak observed in strongly exchange coupled molecular nanomagnets.[10] This is consistent with the simple paramagnetic behavior observed in the magnetization measurements. One can conclude that the spin dynamics reflects the fluctuations of the single magnetic moments of the ions in the molecule without effects associated to the collective spin dynamics except for the very low T region where an upturn of $1/T_1$ is observed for the FM coupled Cu_6Fe and a downturn of $1/T_1$ is observed in AFM coupled Cu_6Co (see inset of Fig. 11). The weak decrease in the relaxation rate in the intermediate temperature range is most likely due to the decrease in spin-diffusion time due to the inhomogeneous broadening of the proton NMR line.[15]

A more quantitative analysis of the data can be done on the basis of Moriya's theory for NSLR in Heisenberg isotropic three-dimensional paramagnets.[16,17] In three-dimensional paramagnets the spectral density $J(\omega)$ of the electronic spin fluctuation is a Lorentzian with a correlation frequency given by[12]

$$\omega_{\text{exc}} = \frac{Jk_B}{\hbar}\sqrt{2zs(s+1)}, \tag{6}$$

where z is the number of nearest neighbors and, for both the systems Cu_6Fe and Cu_6Co, $z=1$.

The NSLR is proportional to the spectral density at both the electronic Larmor frequency ω_e and at the nuclear Larmor frequency ω_n (Refs. 10, 16, and 17)

$$\frac{1}{T_1} = \frac{(\hbar\gamma_e\gamma_n)^2}{4\pi g^2\mu_B^2}k_BT\chi(0)\left[\frac{1}{2}A^{\pm}J^{\pm}(\omega_e) + A^zJ^z(\omega_n)\right], \tag{7}$$

where $A^{\pm}$ and A^z are the Fourier transforms of the spherical component of the product of two dipolar interaction tensors describing the hyperfine coupling of a given proton to the paramagnetic ion along transverse and longitudinal directions, respectively, with respect to the external magnetic field averaged over all protons and all directions.[10,16]

In three-dimensional paramagnets with strong exchange interaction J, the exchange frequency ω_{exc} is much larger

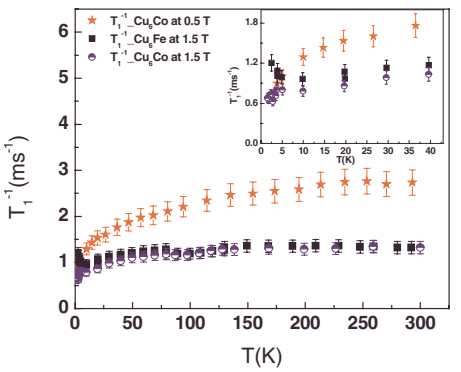

FIG. 11. (Color online) Temperature dependence of spin-lattice relaxation rate at $H=1.5$ T in Cu_6Fe and at $H=1.5$ and 0.5 T in Cu_6Co. The inset shows the low-temperature behavior.

than both ω_e and ω_n and thus one finds that the relaxation rate is field independent since $J^{\pm}(\omega_e)=\frac{\omega_{exc}}{\omega_{exc}^2+\omega_e^2}\cong\frac{1}{\omega_{exc}}$ and $J^z(\omega_n)=\frac{\omega_{exc}}{\omega_{exc}^2+\omega_n^2}\cong\frac{1}{\omega_{exc}}$. On the other hand in the present case, since the exchange coupling is very small, a field dependence is possible from the first term in Eq. (7).

We have fitted the results in Figs. 9 and 10 with Eq. (7) which can be rewritten for a Lorentzian spectral density and $\omega_{exc} \gg \omega_n$ as

$$\frac{1}{T_1}=K\left[\frac{1}{2}A^{\pm}\frac{\omega_{exc}}{\omega_{exc}^2+\omega_e^2}+A^z\frac{1}{\omega_{exc}}\right]. \quad (8)$$

The constant K can be estimated from the known value of the susceptibility $\chi(0)$. The values are $K=1.7$ ms^{-1} for Cu_6Fe and $K=1.4$ ms^{-1} for Cu_6Co. The exchange frequency should be on the order of the value obtained using Moriya's formula[16,17] by using the measured exchange interactions J i.e., $\omega_{exc}=1.3\times10^{10}$ Hz for Cu_6Fe ($J=0.14$ K, ferromagnetic) and $\omega_{exc}=1.036\times10^{11}$ Hz for Cu_6Co ($J=-1.12$ K, antiferromagnetic).

The experimental data in Figs. 10 and 11 can be fitted by Eq. (8) with values for the hyperfine constants: $A^{\pm}\cong1.4\times10^{46}$ cm^{-6} and $A^z\cong0.31\times10^{46}$ cm^{-6} for Cu_6Fe and $A^{\pm}\cong2.07\times10^{46}$ cm^{-6} and $A^z\cong0.4\times10^{46}$ cm^{-6} for Cu_6Co. The fitting parameters are of the correct order of magnitude as obtained in the case of many other molecular nanomagnets.[10,18] In particular, the values of A^z, which depend only on the tensorial dipolar interaction,[9] are consistent with a dipolar interaction of protons with nearest-neighbor and next-nearest-neighbor magnetic ions. The coupling constant $A^{\pm}$, on the other hand, can contain contributions from both the dipolar interaction and the scalar contact hyperfine interaction. In both cases we found that $A^{\pm}>A^z$, which is an indication of the presence of an additional contribution due to a contact interaction arising from the hybridization of hydrogen s wave function with the d wave function of Cu ions as found in the analysis of the spectra (see Sec. III C). The exchange frequencies which best fit the data are: (a) for Cu_6Fe, 1.0×10^{11} Hz, 1.3×10^{11} Hz and 1.4×10^{11} Hz at 300, 77, and 4.2 K, respectively, (b) for Cu_6Co, 1.2×10^{11} Hz, 1.7×10^{11} Hz, 1.9×10^{11} Hz for 300, 77, and 4.2 K, respectively. In both cases the estimated error is $\pm10\%$. The weak temperature dependence is probably irrelevant since the recovery of the nuclear magnetization and thus the value of the measured NSLR can be affected in a different way at different temperatures by spin-diffusion effects which are too difficult to account for. The order of magnitude of the exchange frequency extracted from the data is in excellent agreement with the theoretical value from Moriya's Eq. (6) ($\omega_{exc}=1.036\times10^{11}$ Hz) only for Cu_6Co. For Cu_6Fe the experimental value is one order of magnitude larger. This could be due to a much faster fluctuation rate for the Fe^{3+} magnetic moment as also suggested by the impossibility of detecting the EPR signal.

IV. SUMMARY AND CONCLUSIONS

We have shown that Cu_6Fe and Cu_6Co are novel magnetic molecular clusters in the sense that, contrary to most of the molecular nanomagnets,[1] the magnetic centers are very weakly coupled within the cluster. Thus a crystal of Cu_6Fe (Cu_6Co) is made up of identical single-molecule paramagnets. In Cu_6Fe the Cu^{2+} ions ($s=1/2$) are found to be coupled in pairs via the magnetic Fe^{3+} ($s=1/2$) ion by a superexchange ferromagnetic interaction with $J_F=0.14$ K. In view of the weakness of the coupling constant it could also be a simple dipolar coupling between the Cu^{2+} ion and the Fe^{3+} ion. On the other hand in Cu_6Co, the Cu^{2+} ions appear to be coupled via the diamagnetic Co^{3+} ion by a superexchange antiferromagnetic interaction with $J_{AF}=-1.12$ K.

In both compounds the EPR spectra are indicative of an octahedral Cu^{2+} site with axial distortion (i.e., $g_{\parallel}=2.172$ and $g_{\perp}=2.085$). The proton spin-lattice relaxation time is consistent with an almost temperature-independent single correlation frequency $\omega_{exc}=10^{11}$ Hz related to the fluctuations of the electron spin due to the T_2-type flip-flop transitions associated to the weak exchange coupling as predicted by Moriya.[16,17] However, a quantitative disagreement with the simple Moriya's prediction is found for Cu_6Fe for which we cannot find the EPR signal of the Fe^{3+} ion, a circumstance which suggests a fast fluctuation of this ionic magnetic moment not accounted for by Moriya's theory, which applies to the isotropic Heisenberg interactions only. Below about 2 K the proton relaxation rate shows an increase in Cu_6Fe due to the ferromagnetic correlations and a decrease in Cu_6Co due to antiferromagnetic correlations (see inset Fig. 11). Measurements at much lower temperature are necessary to investigate the possible presence of long-range magnetic order.

In conclusion the magnetic molecular clusters studied here appear to be very suitable candidates to investigate magnetic ordering at very low temperature (millikelvin range) where the competition between the weak intramolecular exchange interaction and the even weaker intermolecular dipolar interaction may lead to some novel kind of magnetic order.

ACKNOWLEDGMENTS

We acknowledge support from the EU Network of Excellence MAGMANet and from Grant PRIN N.2006029518 of the Italian Ministry of Research.

*Corresponding author; lascialfari@fisicavolta.unipv.it

[1] D. Gatteschi, R. Sessoli, and J. Villain, *Molecular Nanomagnets* (Oxford University Press, New York, 2006).

[2] M. N. Leuenberger and D. Loss, Nature (London) **410**, 789 (2001).

[3] F. Troiani, M. Affronte, S. Carretta, P. Santini, and G. Amoretti, Phys. Rev. Lett. **94**, 190501 (2005).

[4] C. Maxim, M. Andruh, A. Lascialfari, M. Marinone, P. Khuntia,

and L. Sorace (unpublished).
[5] M. Atanasov, P. Comba, S. Forster, G. Linti, T. Malcherek, R. Miletich, A. I. Prikhod'ko, and H. Wadepohl, Inorg. Chem. **45**, 7722 (2006).
[6] M. Atanasov, C. Busche, P. Comba, F. El Hallak, B. Martin, G. Rajaraman, J. van Slageren, and H. Wadepohl, Inorg. Chem. **47**, 8112 (2008).
[7] M. Atanasov, P. Comba, Y. D. Lampecka, G. Linti, T. Malcherek, R. Miletich, A. I. Prikhod'ko, and H. Pritzkow, Chem.-Eur. J. **12**, 737 (2006).
[8] S. Golhen, L. Ouahab, D. Grandjean, and P. Molinie, Inorg. Chem. **37**, 1499 (1998).
[9] A. Abragam, *The Principles of Nuclear Magnetism* (Clarendon, Oxford, 1961).
[10] F. Borsa, A. Lascialfari, and Y. Furukawa, in *Novel NMR and EPR Techniques*, edited by J. Dolinsek, M. Vilfan, and S. Zumer (Springer, New York, 2006).
[11] G. C. Carter, L. H. Bennett and D. J. Kahan, *Metallic Shifts in NMR Part 1*, (Pergamon, Oxford, London, 1971).
[12] J. F. Babb and A. Dalgarno, Phys. Rev. A **46**, R5317 (1992).
[13] C. P. Slichter, *Principles of Magnetic Resonance* (Springer-Verlag, Berlin, 1990), p. 131.
[14] M. Belesi, A. Lascialfari, D. Procissi, Z. H. Jang, and F. Borsa, Phys. Rev. B **72**, 014440 (2005).
[15] I. J. Lowe and D. Tse, Phys. Rev. **166**, 279 (1968).
[16] T. Moriya, Prog. Theor. Phys. **28**, 371 (1962).
[17] T. Moriya, Prog. Theor. Phys. **16**, 23 (1956).
[18] A. Lascialfari, D. Gatteschi, F. Borsa, A. Shastri, Z. H. Jang, and P. Carretta, Phys. Rev. B **57**, 514 (1998).